Assessment of the ^{153}Eu and ^{154}Eu neutron capture cross sections from the Integral Data Assimilation of spent nuclear fuel experiments

A. Rizzo, C. Vaglio-Gaudard, G. Noguere, R. Eschbach, J-F. Martin, G. Grassi

Assessment of the ^{153}Eu and ^{154}Eu neutron capture cross sections from the Integral Data Assimilation of used nuclear fuel experiments

Axel RIZZO, Claire VAGLIO-GAUDARD, Gilles NOGUERE, Romain ESCHBACH

CEA, DEN Cadarache, F-13108 Saint Paul les Durance, France

Julie-Fiona MARTIN, Gabriele GRASSI

Orano Cycle, BU Recyclage – Paris, France

ABSTRACT

The purpose of this paper is to make the most of a large set of used nuclear fuel experiments for determining integral trends on the ^{153}Eu(n,γ) and ^{154}Eu(n,γ) reactions cross sections. The assimilation of the integral trends is based on a linear least-square fitting procedure relying on the Bayes' theorem. Realistic uncertainties are obtained thanks to a marginalization technique. The method is applied to the ^{153}Eu and ^{154}Eu capture cross sections recommended in the evaluated nuclear data library JEFF-3.1.1. Our results indicate an underestimation of both capture cross-sections of approximately 4.9% and 7.1%, respectively. For ^{153}Eu, our study suggests to increase the capture resonance integral from I_0=1409 barns to I_0=1502 ± 68 barns. This trend is consistent with the capture resonance integral I_0=1560 barns obtained from recent time-of-flight measurements carried out at the Renssealer Polytechnic Institute. The trend obtained in this work on ^{154}Eu capture cross section is also consistent with a recent analysis carried out on ENDF/B-VII.1, for which ^{154}Eu capture cross section is very similar to JEFF-3.1.1, therefore confirming its underestimation.

Keywords: Nuclear data, DARWIN2.3, CONRAD, Integral data assimilation, ^{153}Eu, ^{154}Eu, capture cross section.

1. INTRODUCTION

The europium isotopes are fission products of interest for nuclear applications. As shown in Fig. 1, ^{153}Eu and ^{154}Eu have a high capture cross-section in the thermal and epi-thermal energy ranges. The main international evaluated nuclear data libraries (JEFF, ENDF/B, JENDL) recommend nearly similar capture cross sections for ^{153}Eu and ^{154}Eu. As indicated in Table 1, the discrepancies between the capture resonance integrals lie below 4%. However, new time-of-flight experiments [1] carried out at the LINAC facility of the Rensselaer Polytechnic Institute (RPI) suggest increasing the ^{153}Eu capture resonance integral of JEFF-3.1.1 [2] by at least 11%. For ^{154}Eu, analyses of Post-Irradiation Examinations (PIEs) in light and heavy water reactors reported in Ref. [3] also suggest increasing the ^{154}Eu capture cross section recommended in the ENDF/B-VII.1 library.

The aim of the present work is to confirm the integral trends reported on the ^{153}Eu(n,γ) and ^{154}Eu(n,γ) reactions by using a large set of used nuclear fuel experiments performed in typical Pressurized Water Reactors (PWRs) energy spectra. The selected integral trends are those calculated with the DARWIN2.3 package [4]. DARWIN2.3 is the French reference calculation package for fuel cycle studies that computes physical quantities of interest for the fuel cycle, at any irradiation and cooling time. The originality of our study is to combine the Integral Data Assimilation procedure and the marginalization technique, implemented in the nuclear data code CONRAD [5,6], for determining integral trends on the ^{153}Eu and ^{154}Eu capture cross sections by taking into account most sources of uncertainties: the uncertainties considered for the study are the ones associated with nuclear data, the ones associated with the interpretation of the PIEs with DARWIN2.3, and uncertainties that account for methodological approximations introduced by DARWIN2.3 deterministic solvers.

The DARWIN2.3 package will be presented in section 2, as well as the experimental data employed for the assimilation and the method used to compute an experimental correlation matrix. The fitting and marginalization techniques used in this work will be presented in section 3. The results will be presented and discussed in section 4.

2. FUEL INVENTORY CALCULATION WITH DARWIN2.3

This section gives a short presentation of both the DARWIN2.3 package and the used nuclear fuel experiments employed in the present study.

2.1. Presentation of the DARWIN2.3 package

DARWIN2.3 [4] is the French reference calculation tool used for fuel cycle studies. It solves the Boltzmann and Bateman equations to compute fuel cycle parameters, at any irradiation and cooling time. The quantities of interest for the fuel cycle are fuel inventory, masses, residual decay heat, neutron emissions, α, ß, γ sources and spectra, and radiotoxicity. A flow chart of the DARWIN2.3 package for PWR calculations is presented in Fig. 2. For PWRs, DARWIN2.3 includes the APOLLO2 deterministic transport code [7], which provides neutron data to the PEPIN2 depletion solver [8]. These data are self-shielded cross-sections libraries and neutron fluxes.

The nuclear data used in the DARWIN calculations come from the JEFF-3.1.1 library. For the multigroup nuclear data, a spatial self-shielding calculation is carried out with the SHEM group structure (281 groups) [9]. The neutron flux is computed with a Probability Collision

method-based calculation. Self-shielded cross-sections and neutron flux are re-calculated as a function of the burnup in order to take into account the impact of the fission products and actinides production.

2.2. Experimental database

The material balance and decay heat calculations with the DARWIN2.3 package have been experimentally validated for PWR [4]. For the material balance, this experimental validation relies on the analysis of dedicated PIEs, mostly consisting in the chemical characterization of in-pile irradiated fuel samples. In this work, the experimental results come from portions of fuel rods extracted from four power reactors, namely Gravelines, Bugey, Dampierre (operated by EdF) and Gösgen (operated by Kernkraftwerk Gösgen-Däniken). The calculated-to-experimental ratios of interest for the ^{153}Eu and ^{154}Eu build-up are reported in Table 2. The associated uncertainties account for the experimental uncertainties of the isotopic ratio measurements as well as systematic uncertainties related to the fuel temperature (±50°C), to the moderator temperature (±2°C) and to the burnup scaling procedure (±2%) [4].

2.3. Numerical biases

DARWIN2.3 is a package relying on deterministic calculation schemes and solvers. Methodological approximations, such as self-shielding calculation, spatial discretization and scattering anisotropy, may introduce numerical biases on the computed physical quantities. In this work, specific studies were carried out to provide an order of magnitude on the numerical biases by comparison to a new Monte-Carlo procedure for calculating the evolution of used fuel as a function of burnup as well as numerical biases induced by the new treatment of the

up-scattering resonance effect. Results obtained from these two studies are discussed hereafter.

Comparative pin-cell depletion calculations were carried out between the deterministic code APOLLO2 and the Monte-Carlo code TRIPOLI-4 [10]. They use the same filiation chain optimized for reactivity calculations. Recent developments enables the coupling between TRIPOLI-4 and the MENDEL [11] deterministic depletion solver for performing depletion calculations [12-15]. The independent replicas method is used, meaning that N random seeds are used in order to perform the same depletion calculation N times. The concentration value and its associated uncertainty are derived from the two first moments of the distribution of the N concentration values. The comparative study between APOLLO2 and TRIPOLI-4 was carried out with various fuels, each of them being representative (*i.e.* having the same initial composition) of the PIEs presented in Table 2. Table 3 shows the differences between APOLLO2 and TRIPOLI-4 pin-cell calculations for ^{153}Eu and ^{154}Eu concentration as a function of burnup. One can observe that the resulting differences lie below 1% and remain nearly constant with the burnup. The quoted uncertainties are low. They were obtained with 64 independent replicas. Such low uncertainties should be handled with care: it has been shown that in some specific cases, the independent replicas method could propagate numerical biases along the successive transport / depletion steps [16]. These possible numerical biases are not taken into account by the statistical uncertainty reported in Table 3.

An additional study was performed to investigate the resonant up-scattering effect [17] on fuel inventory calculations. This physical effect is accounted for in APOLLO2 through a dedicated nuclear data library. Table 4 reports the differences between two APOLLO2 pin-cell calculations performed with and without the resonant up-scattering effect. It can be observed that the differences increase with the burnup. For the ^{154}Eu build up, the differences between the two

APOLLO2 calculations become close to 1% above 60 GWd/t.

These two studies made it possible to quantify numerical biases related respectively to the use of deterministic solvers and to the up-scattering effect. In the following section, these numerical biases are considered as additional sources of systematic uncertainties.

2.4. Correlation matrix between calculated-to-experimental ratios

The calculated-to-experimental ratios reported in Table 2 share the same sources of systematic uncertainties (section 2.2) and numerical biases (section 2.3). We have used the AGS method [18] to compute the correlation matrix M_E between the C/E-1 values. The originality of the AGS method is to combine statistical and systematic uncertainties as follows:

$$M_E = D + S.S^T, \tag{3}$$

in which D is a $n \times n$ diagonal matrix containing variances of the uncorrelated uncertainties, and S is a $n \times m$ rectangular matrix containing the systematic uncertainties for each of the $j \in [\![1, m]\!]$ sources of uncertainty. No correlation between the experimental isotopic ratios was provided alongside the results of the chemical analyses. Therefore, the D-matrix only contains the experimental uncertainties coming from the Inductively Coupled Plasma Mass Spectrometry (ICP-MS) technique:

$$D = diag\{var(E_1), var(E_2), \dots, var(E_n)\}, \tag{4}$$

in which $var(E_i)$ represents the uncertainty associated with the i^{th} experiment. For the S-matrix, we have considered four sources of systematic uncertainties:

$$S = \begin{pmatrix} \Delta_{1,1} & \Delta_{2,1} & \Delta_{3,1} & \Delta_{4,1} \\ \vdots & \vdots & \vdots & \vdots \\ \Delta_{1,n} & \Delta_{2,n} & \Delta_{3,n} & \Delta_{4,n} \end{pmatrix}, \tag{5}$$

with:

$$\Delta_{j,i} = \frac{\partial c_i}{\partial p_j} \Delta p_j . \quad (6)$$

Parameters p_1 and p_2 are related to the (1) fuel and (2) moderator temperatures. Their respective contributions $\Delta_{1,i}$ and $\Delta_{2,i}$ were deduced from direct perturbations in the DARWIN calculations. Parameters p_3 and p_4 are related to both numerical biases investigated in section 2.3. Their corresponding contributions $\Delta_{3,i}$ and $\Delta_{4,i}$ are deduced from values reported in Tables 3 and 4.

Fig. 4 shows the final correlation matrix between the calculated-to-experimental ratios obtained with Eq. (3). As expected, non-negligible correlations exist between the various concentration ratios confirming the need of using M_E in the Integral Data Assimilation procedure.

3. INTEGRAL DATA ASSIMILATION PROCEDURE

The Integral Data Assimilation procedure, as implemented in the CONRAD code [5,6], consists in adjusting neutron cross-sections on a given set of calculated-to-experimental ratios and in propagating statistical and systematic uncertainties *via* a two-step calculation sequence. The first step is a standard least-square fitting procedure, and the second step is a marginalization procedure that aims at accounting for nuisance parameters uncertainties.

3.1 Model parameters

In this work, free parameters are the ^{153}Eu and ^{154}Eu capture cross sections. They will be adjusted with the CONRAD code in order to improve the calculated-to-experimental ratios reported in Table 2. To avoid the resolution of underestimated systems, capture cross sections were averaged over the neutron flux ϕ. Throughout the paper, 1-group cross-sections are defined

as follows:

$$\bar{\sigma}_{\gamma} = \frac{\int_0^{+\infty} \sigma_{\gamma}(E)\phi(E)dE}{\int_0^{+\infty} \phi(E)dE}, \tag{8}$$

and the 2-group representation is given by:

$$\bar{\sigma}_{\gamma,1} = \frac{\int_0^{E_c} \sigma_{\gamma}(E)\phi(E)dE}{\int_0^{E_c} \phi(E)dE}, \tag{9}$$

$$\bar{\sigma}_{\gamma,2} = \frac{\int_{E_c}^{+\infty} \sigma_{\gamma}(E)\phi(E)dE}{\int_{E_c}^{+\infty} \phi(E)dE}, \tag{10}$$

where E_c=0.5 eV represents the cadmium cut-off energy which is used to calculate the capture resonance integral:

$$I_0 = \int_{E_c}^{+\infty} \frac{\sigma_{\gamma}(E)}{E} dE. \tag{11}$$

As a consequence, the 2-group description of the neutron cross sections will provide useful information on the capture resonance integral. The method is discussed in section 4.2.

The final uncertainties on the 1-group or 2-group cross sections depend on the complex formation chain of the europium isotopes. The latter is illustrated in Fig. 3. The CYRUS tool [19] was used to provide an exhaustive list of nuclear data involved in the ^{153}Eu and ^{154}Eu build-up. The 1-group cross-sections, fission yields, and decay constants of interest for this work are listed in Table 6. Parameter $y_c(X, A)$ represents the thermal cumulative fission yield of nuclide X for actinide A and $\tau(X)$ is the decay period of X. All these parameters are nuisance parameters whose uncertainties are taken either from the covariance database COMAC-V2.0 [20,21], developed at the CEA Cadarache, or from the evaluated nuclear data library JEFF-3.1.1. These uncertainties are marginalized after the fitting procedure.

3.2 Fitting procedure

The fitting algorithm implemented in the CONRAD code [22] relies on the Bayes' theorem:

$$P(\vec{x}|\vec{E},U) = \frac{P(\vec{x},U)\ .\ P(\vec{E}|\vec{x},U)}{\int P(\vec{x},U)\ .\ P(\vec{E}|\vec{x},U)d\vec{x}}\ , \tag{12}$$

where $\vec{x}$ contains the free model parameters, $\vec{E} = (E_1 \cdots E_n)^T$ represents the experimental values, U denotes the prior information, $P(\vec{x},U)$ is the prior probability density of $\vec{x}$, $P(\vec{E}|\vec{x},U)$ is the likelihood probability density, corresponding to the calculated-to-experimental ratios, and $P(\vec{x}|\vec{E},U)$ represents the posterior probability density of $\vec{x}$. Vector $\vec{x}$ can contain the 1-group cross sections defined by Eq. (8):

$$\vec{x} = \left(\bar{\sigma}_\gamma\left(^{153}Eu\right), \bar{\sigma}_\gamma\left(^{154}Eu\right)\right)^T . \tag{13}$$

Alternatively, we can use the 2-group representation to get integral trends on the ^{153}Eu capture cross section above the cadmium cut-off energy (Eq. (10)):

$$\vec{x} = \left(\bar{\sigma}_{\gamma,2}\left(^{153}Eu\right), \bar{\sigma}_\gamma\left(^{154}Eu\right)\right)^T . \tag{14}$$

Few assumptions are needed in order to find the two first moments of $P(\vec{x}|\vec{E},U)$. According to the principle of maximum entropy, a multivariate joint normal distribution can be chosen for the prior probability density. If the Laplace approximation is made, the posterior density probability is also assumed to be a normal distribution. Then, the posterior parameters $\vec{x}_m$ and covariance matrix M_x correspond to the minimum of the following cost function:

$$\chi^2{}_{GLS} = (\vec{x}-\vec{x}_m)^T M_x^{-1}(\vec{x}-\vec{x}_m) + (\vec{C}-\vec{E})^T M_E^{-1}(\vec{C}-\vec{E})\ , \tag{15}$$

in which $\vec{C} = (C_1 \cdots C_n)^T$ contains the calculated values and M_E is the experimental correlation matrix (section 2.4). A Gauss-Newton iterative scheme [22] is normally used to solve Eq. (15), ensuring a good convergence of the minimizing process in spite of the non-linearity of this equation when adjusting resonance parameters of a cross section for instance. In this study,

the problem may be considered linear given the number of fitted parameters and the number of experiments. Hence, a single iteration is used in this work, and it gives a global trend on the capture cross section of the europium isotopes that can prove useful for future experimental and evaluation works.

3.3 Marginalization procedure

The marginalization technique [23] was implemented in CONRAD, to account for the uncertainties on nuisance parameters (non-fitted model parameters θ) listed in Table 6. It consists in building a "full" covariance matrix Σ between fitted and nuisance parameters from their M_x and M_θ respective covariance matrices [24]:

$$\Sigma = \begin{pmatrix} M_{x,Marg.} & M_{x,\theta} \\ {M_{x,\theta}}^T & M_\theta \end{pmatrix}, \tag{16}$$

where

$$M_{x,Marg.} = M_x + ({G_x}^T G_x)^{-1} {G_x}^T G_\theta . M_\theta . {G_\theta}^T \, G_x ({G_x}^T G_x)^{-1}, \tag{17}$$

and

$$M_{x,\theta} = -\left({G_x}^T G_x\right)^{-1} {G_x}^T . G_\theta . M_\theta . \tag{18}$$

The M_x-matrix represents the posterior covariance matrix provided by the fitting algorithm. The G_x and G_θ partial derivative matrices contain the derivatives of the calculated values with respect to the fitted and non-fitted parameters:

$$G_x(i,j) = \frac{\partial C_i}{\partial x_j}, \tag{19}$$

$$G_\theta(i,j) = \frac{\partial C_i}{\partial \theta_j}. \tag{20}$$

To avoid Peelle's pertinent puzzle [25], namely the occurrence of abnormal values of quantities fitted on experimental data with both statistical and large systematic uncertainties, it was also

chosen to marginalize the uncertainty associated to the burnup scaling procedure (±2%). This strategy was applied in Ref. [26] to treat the first resonance of ^{239}Pu.

4. RESULTS

The Integral Data Assimilation procedure presented in section 3 was used to extract integral trends on the 1-group capture cross sections of ^{153}Eu and ^{154}Eu (Eq. (13)), and also on the capture resonance integral of ^{153}Eu (Eq. (14)).

4.1 Integral trends on 1-group capture cross sections

Prior uncertainties on the 1-group capture cross sections of ^{153}Eu and ^{154}Eu were calculated from the COMAC-V2.0 covariance database. These prior relative uncertainties are then introduced in the fitting procedure, with values of ±5% for $\bar{\sigma}_\gamma\left(^{153}Eu\right)$ and ±11% for $\bar{\sigma}_\gamma\left(^{154}Eu\right)$. Two series of calculations were performed: one with the fission yield uncertainties coming from COMAC-V2.0 and the other with those from the JEFF-3.1.1 library.

Table 6 shows the final integral trends deduced from the calculated-to-experimental ratios of Table 2. The marginalization procedure provides more realistic uncertainties than the fitting procedure only. One can also observe a slight reduction of the uncertainty of about 1.5% when using the COMAC-V2.0 uncertainties for thermal cumulative fission yields. This is mainly explained by the strong reduction of the uncertainty for the $y_c\left(^{151}Sm, ^{241}Pu\right)$, *i.e.* ^{241}Pu fission yield on ^{151}Sm. The results suggest an increase of both capture cross-sections, as compared to the JEFF-3.1.1 evaluation. The proposed modifications of +4.9% and +7.1% are within the range of the prior uncertainties. Fig. 5 and Fig.6 show that the posterior C/E-1 values are closer

to zero and the associated uncertainties are reduced, especially for the $^{154}Eu/^{238}U$ isotopic ratios. This trend is explained by the strong correlation coefficient of 0.98 between the two fitted parameters.

Table 7 reports some integral trends dedicated to the experimental validation of the ^{153}Eu evaluation available in the JEFF-3.1.1 library. They come from the analysis of oscillation and activation measurements carried out in critical mock-up with PWR-like neutron spectra [26-29]. The negative sign indicate that the ^{153}Eu capture cross section in JEFF-3.1.1 is underestimated. Our results confirm these trends.

Regarding ^{154}Eu capture cross-section, a recent work based on ENDF/B-VII.1 also indicates an overestimation of the ^{154}Eu concentration in Light and Heavy Water Reactors [3]. As indicated in Table 1, the evaluations in JEFF-3.1.1 and ENDF/B-VII.1 are nearly similar. Therefore, conclusions from Ref. [3] are consistent with the calculated-to-experimental ratios of Table 2, and then confirm the sizeable underestimation of the capture cross-section in both libraries.

4.2 Integral trend on the capture resonance integral

In a second step, we tried to discriminate the contribution of the thermal energy range and of the resonance range of the ^{153}Eu capture cross-section using the 2-group representation defined by Eqs (9) and (10). Below 0.5 eV, the 1/v behaviour of the capture cross-section is mainly conditioned by the value at the thermal energy. Therefore, $\bar{\sigma}_{\gamma,1}$ strongly depends on the thermal value σ_0. Similarly, a direct perturbation of $\bar{\sigma}_{\gamma,2}$ could be seen as a perturbation of the capture resonance integral I_0. As shown in Fig. 1, such an approach cannot be applied to ^{154}Eu, because the first resonance is too close to the thermal cross section.

A few experimental values for the ^{153}Eu thermal capture cross section [30-34] are reported in Table 8. They are all in reasonable agreement within the uncertainties range, confirming the JEFF-3.1.1 value of σ_0=312 barns. Therefore, we decided to adjust $\bar{\sigma}_{\gamma,2}$ and to marginalize the uncertainty of $\bar{\sigma}_{\gamma,1}$ together with the uncertainties of the nuisance parameters listed in Table 5. For $\bar{\sigma}_{\gamma,1}$, we use the relative uncertainty that corresponds to the standard deviation of the experimental values depicted in Table 8, which is approximately 5%. For $\bar{\sigma}_{\gamma,2}$, its prior relative uncertainty was deduced from COMAC-V2.0, with a value close to 7%.

If the fission yield uncertainties of JEFF-3.1.1 are introduced in the marginalization procedure of the nuisance parameters (Table 8), the two-step CONRAD calculation provides the following trends for ^{153}Eu and ^{154}Eu:

$$\Delta\bar{\sigma}_{\gamma,2}(^{153}\text{Eu}) = + (6.6 \pm 6.8)\ \%,$$

$$\Delta\bar{\sigma}_{\gamma}(^{154}\text{Eu}) = + (6.7 \pm 7.4)\ \%.$$

When the fission yields uncertainties of COMAC-V2.0 are used, we obtain smaller uncertainties:

$$\Delta\bar{\sigma}_{\gamma,2}(^{153}\text{Eu}) = + (6.6 \pm 4.8)\ \%,$$

$$\Delta\bar{\sigma}_{\gamma}(^{154}\text{Eu}) = + (6.7 \pm 5.9)\ \%.$$

Both results still suggest an increase of JEFF-3.1.1 capture cross sections. The integral trend for the ^{154}Eu(n,γ) reaction remains consistent with the previous trends (+7.1%) reported in Table 6, while the trend for the ^{153}Eu(n,γ) reaction between 0.5 eV to 20 MeV is slightly higher than the one given in Table 6 (+4.9%), which is obtained for the whole neutron energy range. Assuming that modifying the ^{153}Eu(n,γ) reaction by $\Delta\bar{\sigma}_{\gamma,2}(^{153}\text{Eu})$ is nearly equivalent to modifying the capture resonance integral I_0, then $\Delta\bar{\sigma}_{\gamma,2}(^{153}\text{Eu})$ corresponds to an increase of the capture

resonance integral of JEFF-3.1.1 from I_0=1409 barns to $I_0 \approx$1502 ± 96 barns **(**using the fission yields uncertainties of JEFF-3.1.1), or to $I_0 \approx$1502 ± 68 barns (using the fission yields uncertainties of COMAC-V2.0). This tendency is in good agreement with the I_0 = 1560 barns value deduced from the time-of-flight data measured at the Rensselaer Polytechnic Institute [1]. Such an agreement confirms our choice to marginalize the uncertainties of $\bar{\sigma}_{\gamma,1}$ and to apply the calculated-to-experimental biases on the ^{153}Eu capture resonance integral of JEFF-3.1.1.

5. CONCLUSION

The results obtained in the present work confirm the relevancy of using the fitting algorithm of the CONRAD code in association with the marginalization of the nuisance parameter uncertainties for determining reliable integral trends from PIE analyses. Previous studies with the DARWIN2.3 package of several ^{153}Eu/^{238}U and ^{154}Eu/^{238}U isotopic ratios as a function of the burnup indicated a possible underestimation of the ^{153}Eu and ^{154}Eu capture cross sections recommended in the JEFF-3.1.1 library. The use of the CONRAD algorithms allowed to suggest an increase of (4.9 ± 3.2)% and (7.1 ± 6.0)% of the ^{153}Eu(n,γ) and ^{154}Eu(n,γ) reaction cross sections, respectively. For ^{153}Eu, integral trends of similar amplitude, ranging from 6% to 11.6%, were reported in the literature.

Characteristics of the ^{153}Eu capture cross section allow distinguishing the contribution of the thermal and epithermal energy ranges. Since the ^{153}Eu thermal cross-section recommended in JEFF-3.1.1 (σ_0=312 barns) is in good agreement with the experimental values reported in the literature, we assumed that the calculated-to-experimental biases are mainly due to the underestimation of the ^{153}Eu capture resonance integral in JEFF-3.1.1. The CONRAD calculations suggested to increase by +(6.6 ± 4.8)% the capture resonance integral from 1409

barns to 1502±68 barns. This result is consistent with the capture resonance integral I_0=1560 barns deduced from measurements carried out at the RPI facility. As a consequence, the resonance parameters extracted from the RPI data can be used in the future release of the JEFF library.

ACKNOWLEDGMENTS

We would like to thank all the colleagues from CEA who helped us during this work, especially David Bernard, Coralie Carmouze, Pierre Leconte, Pascal Archier, and Vanessa Vallet.

REFERENCES

[1] G. Leinweber *et al.*, "Europium resonance parameters from neutron capture and transmission measurements in the energy range 0.01-200 eV", *Annals of Nuclear Energy*, **69**, pp74-89 (2014)

[2] A. Santamarina *et al.*, "The JEFF-3.1.1 Nuclear Data library", *JEFF report*, **22**, OECD-NEA data bank (2009)

[3] S. E. Skutnik, "Proposed re-evaluation of the ^{154}Eu thermal (n,γ) capture cross-section based on spent fuel nuclear benchmarking studies", *Annals of Nuclear Energy*, **99**, pp80-107 (2017)

[4] L. San-Felice *et al.*, "Experimental validation of the DARWIN2.3 package for fuel cycle applications", *Nuclear Technology*, **184**, pp217-232 (2013)

[5] C. de Saint Jean *et al.*, "Status of CONRAD, a nuclear reaction analysis tool", Proc. Int. Conf. *Nuclear Data for Science and Technology*, Nice, France (2007)

[6] P. Archier *et al.*, "CONRAD evaluation code: Development Status and Perspectives", Proc. Int. Conf. *Nuclear Data for Science and Technology*, New-York, USA (2013)

[7] A. Santamarina *et al.*, "APOLLO2.8: a validated code package for PWR calculations", Proc.

Int. Conf. *Advances in Nuclear Fuel Management IV*, Hilton Head Island, South Carolina USA (2009)

[8] A. Tsilanizara *et al.*, "DARWIN: an Evolution Code System for a Large Range of Applications", Proc. Int. Conf. *ICRS-9*, Tsukuba, Ibaraki, Japan (1999)

[9] N. Hfaiedh *et al.*¸ "Determination of the Optimized SHEM mesh for neutron transport calculation", Proc. Int. Conf. *M&C* (2009)

[10] E. Brun *et al.*, "TRIPOLI-4®, CEA, EDF, and AREVA reference Monte Carlo code", *Annals of Nuclear Energy*, **82**, pp151-160 (2015)

[11] S. Lahaye *et al.*, "First Verification and Validation steps of MENDEL release 1.0 cycle code system", Proc. Int. Conf. *PHYSOR*, Kyoto, Japan (2014)

[12] F. Damian & E. Brun, "ORPHEE research reactor: 3D core depletion calculation using Monte-Carlo code TRIPOLI-4®", Proc. Int. Conf. *SNA+MC*, Paris, France (2013)

[13] D. Blancher *et al.*, "On core- reflector interface effects in the ASTRID sodium cooled fast reactor", Proc. Int. Conf. *ICAPP*, San Francisco, California, USA (2016)

[14] P. Archier *et al.*, "Validation of a multi-purpose depletion chain for burnup calculations through TRIPOLI-4 calculations and IFP perturbation method", Proc. Ind. Conf *PHYSOR*, Sun Valley, Idaho, USA (2016)

[15] A. Chambon *et al.*, "Validation of HORUS3D/N against TRIPOLI-4®D for code depletion calculation of the Jules Horowitz reactor", Proc. Ind. Conf *PHYSOR*, Sun Valley, Idaho, USA (2016)

[16] E. Dumonteil & C. M. Diop, "Biases and statistical errors in Monte Carlo burnup calculations: an unbiased stochastic scheme to solve Boltzmann/Bateman coupled equations", *Nuclear Science and Engineering*, **167**, pp165-170 (2011)

[17] M. Ouisloumen *et al.*, "A model for neutron scattering off heavy isotopes that accounts for thermal agitation effects", *Nuclear Science and Engineering*, **107**, pp189-200 (1991)

[18] C. Bastian *et al.*, "AGS, a computer code for uncertainty propagation in time-of-flight cross-section data", Proc. Int. Conf. *PHYSOR*, Vancouver, Canada (2006)

[19] V. Vallet *et al.*, "Deterministic approach of the decay heat uncertainty due to JEFF-3.1.1 nuclear data uncertainties with the CYRUS tool and the DARWIN2.3 depletion code", Proc. Int. Conf. *PHYSOR*, Kyoto, Japan (2014)

[20] P. Archier *et al.*, "COMAC – Nuclear data covariance matrices library for reactor applications", Proc. Int. Conf. *PHYSOR*, Kyoto, Japan (2014)

[21] N. Terranova, *Covariance Evaluation for Nuclear Data of Interest to the Reactivity Loss Estimation of the Jules Horowitz Reactor*, Ph.D. thesis report, Bologne University, Italy (2016)

[22] E. Privas *et al.*, "Generation of ^{238}U covariance matrices by using the integral data assimilation technique of the CONRAD code", *EPJ Web of Conferences*, **106**, 04015 (2016)

[23] B. Habert *et al.*, "Retroactive generation of covariance matrix of nuclear model parameters using marginalization techniques", *Nuclear Science and Engineering*, **166**, pp276-287 (2010)

[24] G. Noguere *et al.*, "Zero variance penalty model for the generation of covariance matrices in integral data assimilation problems", *Nuclear Science and Engineering*, **172**, pp164-179 (2012)

[25] D. L. Smith, *Probability, statistics, and data uncertainties in nuclear science and technology*, American Nuclear Society, La Grange Park, Illinois (1991)

[26] C. De Saint Jean *et al.*, "Evaluation of neutron-induced cross sections and their related covariances with physical constraints", *Nuclear Data Sheets*, **148**, pp383-419 (2018)

[27] C. J. Dean *et al.*, "Validation of important fission product evaluations through CERES integral benchmarks", Proc. Int. Conf. *Nuclear Data for Science and Technology*, Nice, France (2007)

[28] A. Gruel *et al.*, "Interpretation of Fission Products Oscillations in the MINERVE reactor, from Thermal to Epithermal Spectra", *Nuclear Science and Engineering*, **169**, pp229-244 (2011)

[29] D. Bernard *et al.*, "Validation of JEFF-3.1.1 Thermal and Epithermal neutron-induced capture cross-sections through MELUSINE experiment analysis", *Nuclear Science and Engineering*, **179**, pp302-312 (2015)

[30] P. Leconte *et al.*, "Thermal neutron activation experiments on Ag, In, Cs, Eu, V, Mo, Zn, Sn and Zr in the MINERVE facility", *EPJ Web of Conferences*, **111**, 07001 (2016)

[31] R. B. Tattersal *et al.*, "Pile oscillator measurements of resonance absorption integrals", *Journal of Nuclear Energy, part A*, **12**, pp32-46 (1960)

[32] M. C. Mowon *et al.*, "The neutron capture cross-section of ^{151}Eu and ^{153}Eu in the energy range 0.1 to 100 keV", *Annals of Nuclear Energy*, **3**, pp399-403 (1976)

[33] F. Farina Arboccò *et al.*, "Experimental determination of k_o, Q_o factors, effective resonance energies and neutron cross-sections for 37 isotopes of interest in NAA", *Journal of Radioanalytical and Nuclear Chemistry*, **302**, pp655-672 (2014)

[34] M. S. Basunia *et al.*, "Determination of the ^{151}Eu(n,γ)^{152m1,g}Eu and ^{153}Eu(n,γ)^{154}Eu reaction cross-sections at thermal neutron energy", *Nuclear Data Sheets*, **119**, pp88-90 (2014)

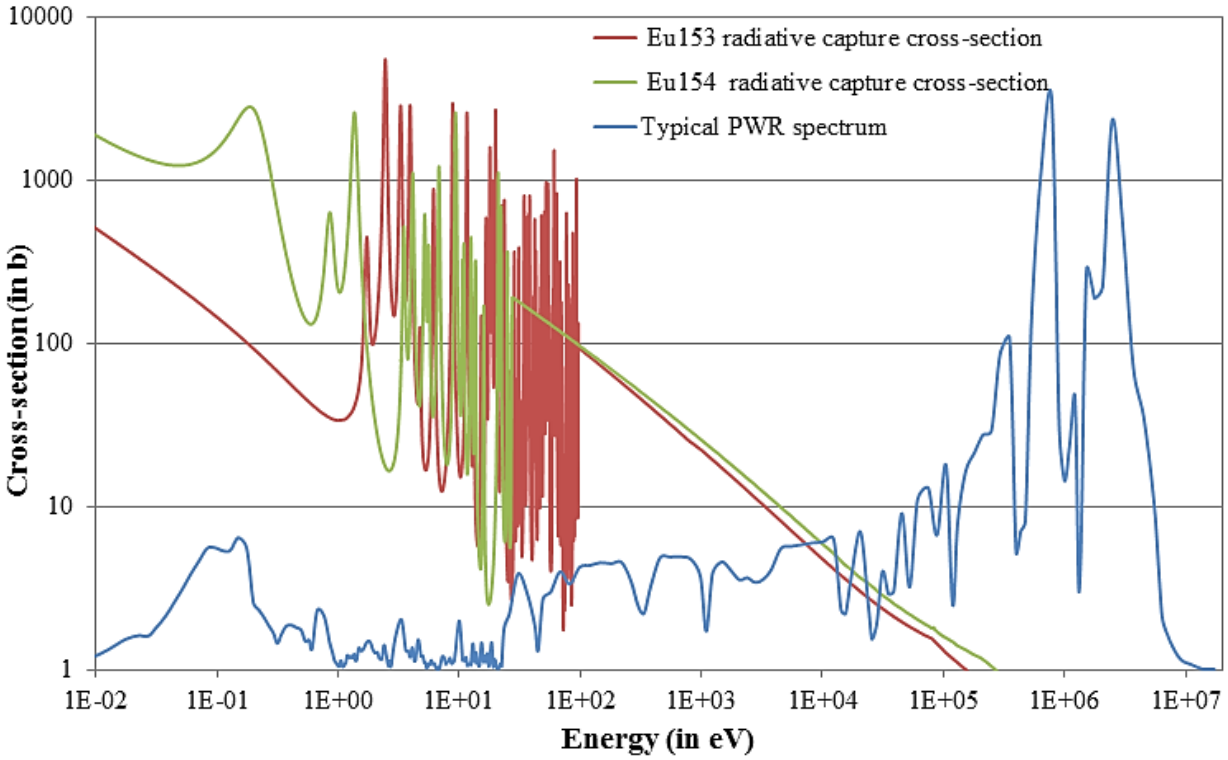

Figure 1. ^{153}Eu and ^{154}Eu radiative capture cross-sections recommended in the evaluated nuclear data library JEFF-3.1.1 compared to a PWR neutron spectrum (in arbitrary unit).

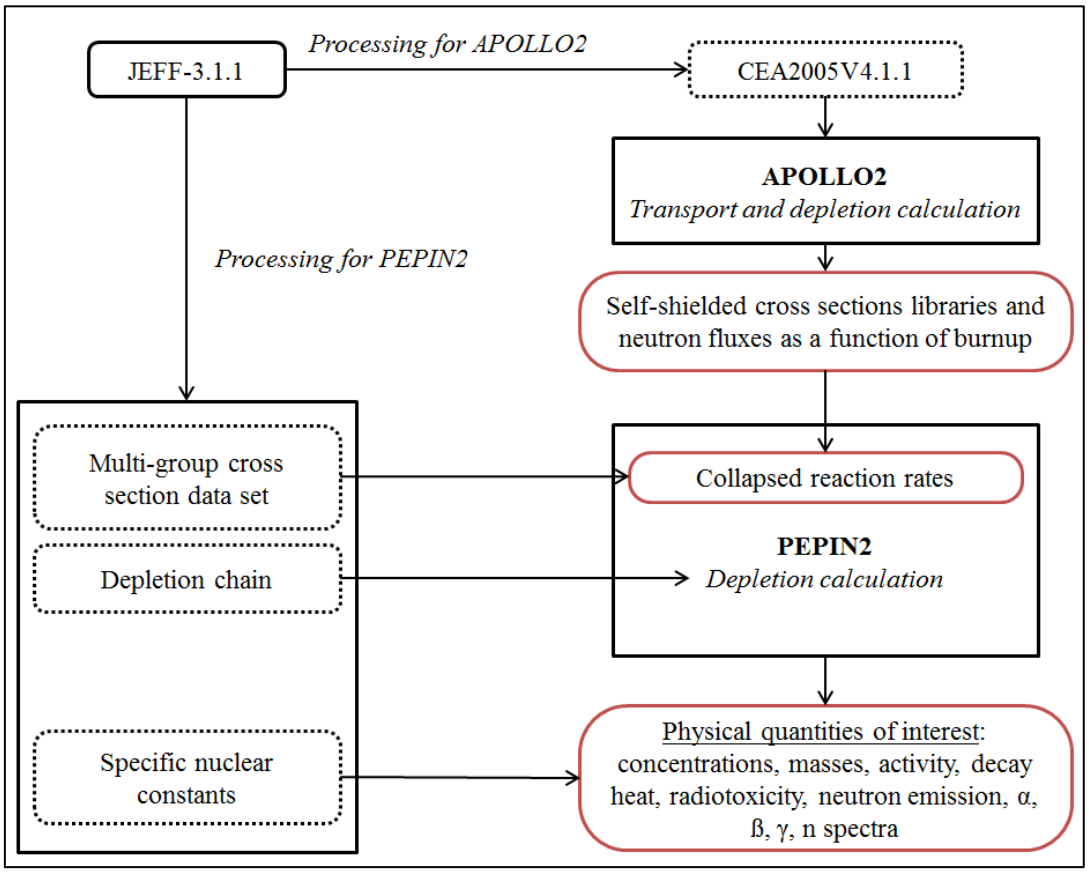

Figure 2. Flow chart of the DARWIN2.3 package for PWR calculations.

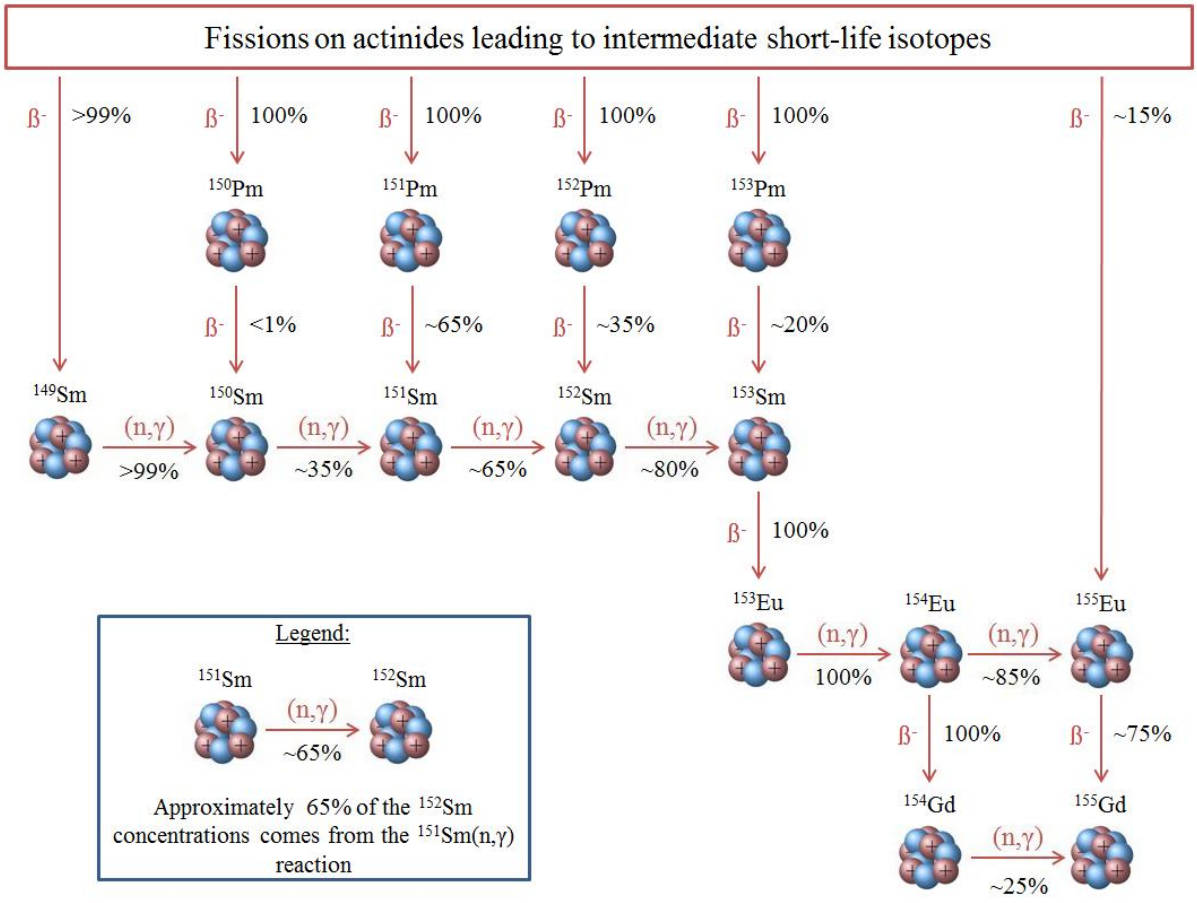

Figure 3. Build up of the ^{153}Eu and ^{154}Eu isotopes in a PWR-like spectrum for a 4.5 wt.% ^{235}U UOX fuel and a 6.7wt.% Pu amount MOX fuel – both of them irradiated at 40 GWd/t – given by the CYRUS tool [19].

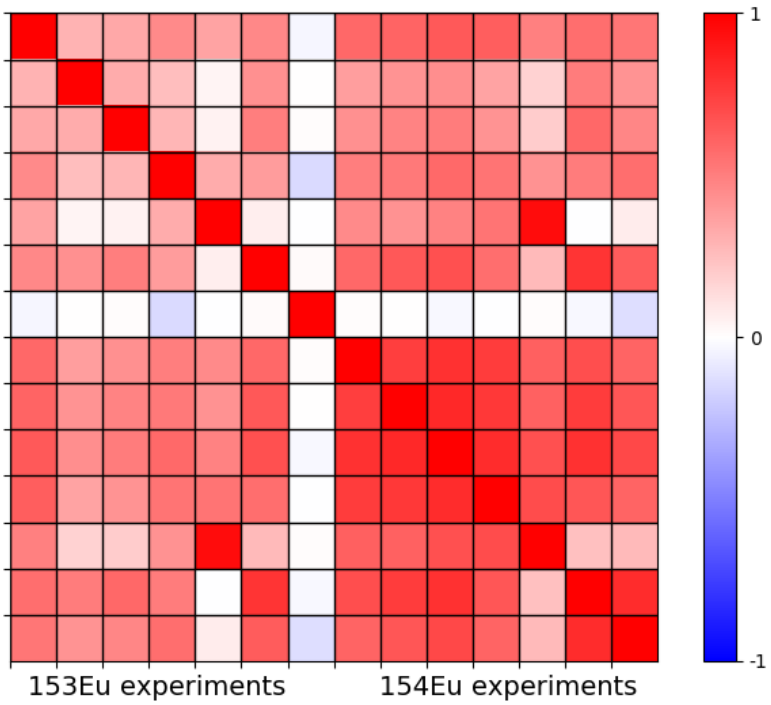

Figure 4. Experimental correlation matrix generated with the AGS method between the 14 calculated-to-experimental ratios reported in Table 2.

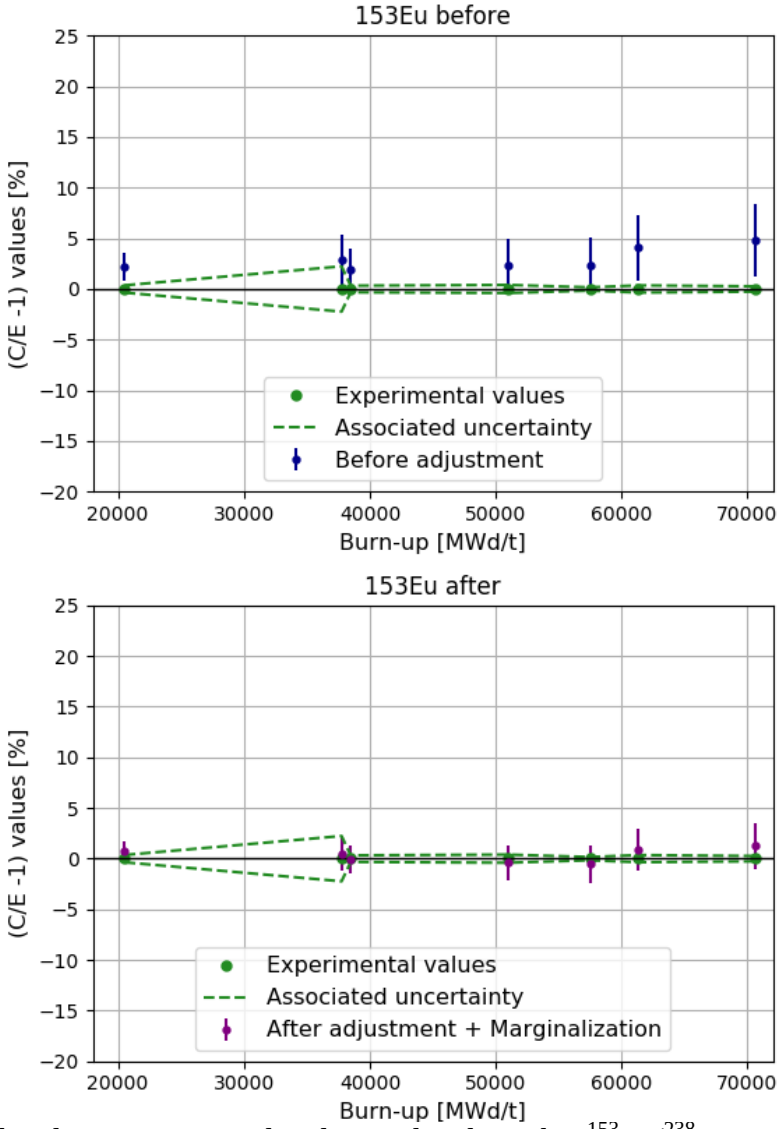

Figure 5. Calculated-to-experimental values related to the ^{153}Eu/^{238}U isotopic ratios before adjustment (top plots) and after adjustment (bottom plots) of the ^{153}Eu and ^{154}Eu 1-group capture cross sections.

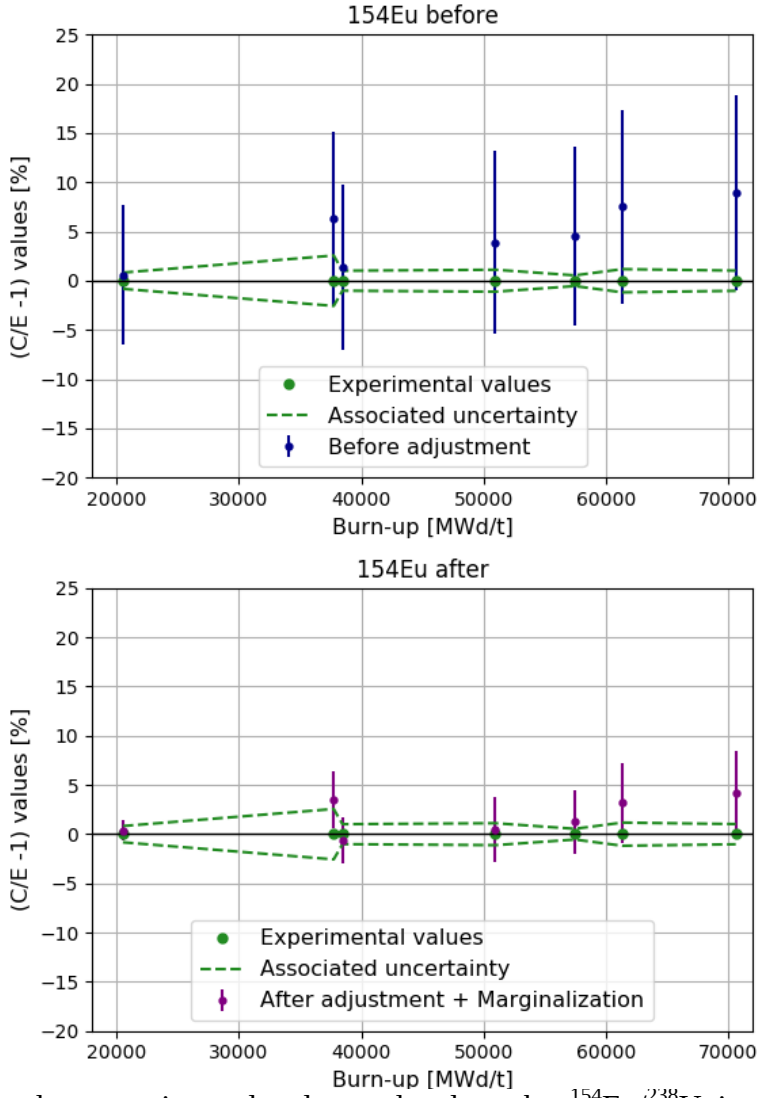

Figure 6. Calculated-to-experimental values related to the $^{154}Eu/^{238}U$ isotopic ratios before adjustment (top plots) and after adjustment (bottom plots) of the ^{153}Eu and ^{154}Eu 1-group capture cross sections.

Table 1. Thermal capture cross section σ_0 and capture resonance integral I_0 of the ^{153}Eu and ^{154}Eu isotopes given in the main international evaluated nuclear data libraries.

Evaluated nuclear data library	^{153}Eu		^{154}Eu	
	σ_0 (barns)	I_0 (barns)	σ_0 (barns)	I_0 (barns)
JEFF-3.1.1	313	1409	1356	1326
ENDF/B-VII.0	312	1409	1353	1299
ENDF/B-VII.1	358	1420	1353	1299
JENDL-4.0	313	1412	1353	1354

Table 2. Calculated-to-experimental ratios related to the $^{153}Eu/^{238}U$ and $^{154}Eu/^{238}U$ isotopic ratios provided by DARWIN2.3 [4], *i.e.* before the adjustment performed in this work. The origins of the relative uncertainties σ are explained in section 2.2.

Reactor name and fuel characteristics	Burnup (GWd/t)	^{153}Eu / ^{238}U		^{154}Eu / ^{238}U	
		C/E-1 (%)	σ (%)	C/E-1 (%)	σ (%)
Gravelines – 4.5% ^{235}U-enriched UOX fuel (17×17 rods)	40 50 60	2.0 2.3 4.1	2.6 2.3 1.9	1.4 3.9 7.5	3.5 2.8 2.3
Bugey – 3.1% ^{235}U-enriched UOX fuel (17×17 rods)	20 25	2.2 2.9	2.9 3.3	0.6 6.3	4.0 3.8
Gösgen – 4.3% ^{235}U-enriched UOX fuel (15×15 rods)	70	4.8	1.6	9.0	1.8
Dampierre – 6.7% Pu amount in the central zone (17×17 rods)	58	2.3	1.2	4.5	2.6

Table 3. Differences obtained on the $^{153}Eu/^{238}U$ and $^{154}Eu/^{238}U$ isotopic ratios between APOLLO2 (AP2) and TRIPOLI-4 (T4) pin-cell calculations as a function of burnup. The relative uncertainties σ_{T4} represent the statistical uncertainties of the Monte-Carlo simulations.

Fuel characteristics used in the pin-cell calculations	Burnup (GWd/t)	^{153}Eu / ^{238}U		^{154}Eu / ^{238}U	
		C(AP2)/C(T4)-1 (%)	σ_{T4} (%)	C(AP2)/C(T4)-1 (%)	σ_{T4} (%)
4.5 wt.% ^{235}U UOX fuel (Gravelines)	40 50 60	0.09 0.10 0.11	0.02 0.02 0.01	0.45 0.47 0.42	0.02 0.02 0.02
3.1% wt.% ^{235}U UOX fuel (Bugey)	20 25	-0.04 0.01	0.02 0.02	0.29 0.37	0.02 0.02
4.3% wt.% ^{235}U UOX fuel (Gösgen)	70	0.11	0.01	0.42	0.02
6.7 wt. % Pu amount MOX (Dampierre)	58	0.06	0.02	-0.21	0.02

Table 4. Differences obtained on the $^{153}Eu/^{238}U$ and $^{154}Eu/^{238}U$ isotopic ratios between two APOLLO2 pin-cell calculations with (AP2-UPS) and without (AP2) up-scattering effects.

Fuel characteristics used in the pin-cell calculations	Burnup (GWd/t)	^{153}Eu / ^{238}U	^{154}Eu / ^{238}U
		C(AP2-UPS)/C(AP2)-1 (%)	C(AP2-UPS)/C(AP2)-1 (%)
4.5 wt.% ^{235}U UOX fuel (Gravelines)	40 50 60	0.19 0.16 0.14	0.64 0.72 0.81
3.1% wt.% ^{235}U UOX fuel (Bugey)	20 25	0.24 0.22	0.54 0.58
4.3% wt.% ^{235}U UOX fuel (Gösgen)	70	0.14	0.81
6.7 wt. % Pu amount MOX (Dampierre)	58	-0.07	0.31

Table 5. Nuisance parameters and relative uncertainties introduced in the marginalization procedure.

Model parameters		Relative uncertainties	Origin of the uncertainties
1-group cross sections	$^{235}U(n,f)$	0.33%	COMAC-V2.0
	$^{238}U(n,\gamma)$	0.85%	COMAC-V2.0
	$^{239}Pu(n,f)$	1.30%	COMAC-V2.0
	$^{239}Pu(n,\gamma)$	2.30%	COMAC-V2.0
	$^{240}Pu(n,\gamma)$	1.90%	COMAC-V2.0
	$^{241}Pu(n,f)$	1.50%	COMAC-V2.0
	$^{241}Pu(n,\gamma)$	3.30%	COMAC-V2.0
	$^{150}Sm(n,\gamma)$	3.10%	COMAC-V2.0
	$^{151}Sm(n,\gamma)$	6.30%	COMAC-V2.0
	$^{152}Sm(n,\gamma)$	2.90%	COMAC-V2.0
Fission yields	$y_c(^{153}Eu, ^{235}U)$	4.8% / 8.3%	JEFF-3.1.1 / COMAC-V2.0
	$y_c(^{153}Eu, ^{239}Pu)$	7.9% / 5.9%	JEFF-3.1.1 / COMAC-V2.0
	$y_c(^{153}Eu, ^{241}Pu)$	57% / 4.0%	JEFF-3.1.1 / COMAC-V2.0
	$y_c(^{152}Sm, ^{235}U)$	1.1%	JEFF-3.1.1
	$y_c(^{152}Sm, ^{239}Pu)$	2.9%	JEFF-3.1.1
	$y_c(^{152}Sm, ^{241}Pu)$	7.3%	JEFF-3.1.1
	$y_c(^{151}Pm, ^{235}U)$	1.7% / 5.5%	JEFF-3.1.1 / COMAC-V2.0
	$y_c(^{151}Pm, ^{239}Pu)$	2.3% / 3.6%	JEFF-3.1.1 / COMAC-V2.0
	$y_c(^{151}Pm, ^{241}Pu)$	28% / 2.8%	JEFF-3.1.1 / COMAC-V2.0
	$y_c(^{149}Pm, ^{235}U)$	2.0%	JEFF-3.1.1
	$y_c(^{149}Pm, ^{239}Pu)$	2.5%	JEFF-3.1.1
	$y_c(^{149}Pm, ^{241}Pu)$	4.9%	JEFF-3.1.1
Decay Data	$\tau(^{154}Eu)$	0.45%	JEFF-3.1.1

Table 6. Trends on the ^{153}Eu and ^{154}Eu 1-group capture cross-sections obtained from the Integral Data Assimilation of the C/E-1 values reported in Table 2. The positive signs indicate an increase of the capture cross section as compared to the JEFF-3.1.1 evaluations.

Type of fitting procedure	^{153}Eu(n,γ)	^{154}Eu(n,γ)	Correlation
a) Fit only	+ (4.9 ± 0.3)%	+ (7.1 ± 0.6)%	0.694
b) Fit + Marginalization (JEFF-3.1.1 Fission Yields)	+ (4.9 ± 4.7)%	+ (7.1 ± 7.5)%	0.978
c) Fit + Marginalization (COMAC-V2.0 Fission Yields)	+ (4.9 ± 3.2)%	+ (7.1 ± 6.0)%	0.984

Table 7. Calculated-to-experimental values related to the ^{153}Eu capture cross section in PWR-like spectra calculated with the JEFF-3.1.1 library. The negative signs indicate an underestimation of the ^{153}Eu capture cross section of JEFF-3.1.1.

Principal author	Year	Ref.	C/E-1
Dean	2007	[27]	-(6.0±4.0)%
Gruel	2011	[28]	-(11.6±2.8)%
Bernard	2015	[29]	-(9.5±4.3)%
Leconte	2016	[30]	-(8.5±1.3)%

Table 8. ^{153}Eu thermal capture cross-section σ_0 reported in the literature. The value recommended in JEFF-3.1.1 is 312 barns (Table 1).

Principal author	Year	Ref.	σ_0	Relative uncertainties
Tattersal	1960	[31]	317 barns	1.6 %
Moxon	1976	[32]	317 barns	4.7 %
Farina Arbocco	2014	[33]	312 barns	1.0 %
Basunia	2014	[34]	335 barns	3.0 %